

Force calibration of a plurality of optical traps by video-based methods

Josep Mas Soler

Grup de Recerca en Òptica Física, Departament de Física Aplicada i Òptica,
Universitat de Barcelona
Martí i Franqués 1, Barcelona 08028, Spain.

E-mail: josepmassoler@gmail.com

Abstract. Several methods have been used for optical trap force calibration, but few of them offer the possibility to simultaneously calibrate multiple traps. In this work a conceptually simple calibration method based on thermal noise analysis by video particle tracking has been implemented. Preliminary results are quite satisfactory, although there are significant discrepancies with other consolidated methods. Advantages and limitations of this method are discussed at the end of this work and further improvements are proposed.

Keywords: Optical tweezers, Force calibration, video tracking, Brownian movement.

1. Introduction

Optical tweezers are highly focused light beams which are able to trap and move little particles (from microns to nanometers size) taking advantage of the radiation pressure. Nowadays optical tweezers are being used in a lot of biophysical experiments like single molecule experiments, molecular motors studies and cellular manipulation [1]. In some cases optical tweezers are used just as a manipulating tool, but they can also be used to exert a controlled force on a microscopic body, or to measure forces involved in biological processes.

Particle acceleration by radiation pressure was first reported by Ashkin [2] in 1970, who was able to trap microscopic spheres using two counter-propagating laser beams. In 1986 optical trapping with a single highly focused laser beam was achieved [3]. The trapping mechanism is based on the momentum exchange between the trapping beam and the trapped particle by a scattering process. The resulting force can be explained with different models depending on the particle size: geometrical optics regime [4] (particle bigger than the laser wavelength), Rayleigh Regime [5] (small particle), or the general approach regime [6].

The net force can be decomposed in a scattering force pushing the bead in the direction of beam propagation, and a gradient force attracting the bead towards higher intensity regions. In order to get a stable trap, gradient force should overcome the scattering force, which happen when there is a high light intensity gradient (it can be obtained by focusing a light beam with a high numerical aperture objective). An important advance for optical tweezers versatility came with holographic optical tweezers, which use wavefront coding techniques to reshape, redirect or divide the trapping beam. Using spatial light modulators for modifying the wavefront one can obtain arbitrary trap distributions [7,8].

Optical tweezers can measure forces like a dynamometer. If the trap is calibrated (optical force is known as a function of the bead position), then it is possible to know which external force is applied by looking at the bead move towards a new equilibrium position (where trap force and external force compensate). Usually trap potential is assumed to be harmonic: $F=-k \cdot x$, and there are several precise and reliable calibration methods to characterize it [9]. A conceptually simple calibration method consists of applying a known force and measuring the displacement of the trapped bead from the trap centre. The applied force is usually a drag force (controlled fluid flow around the trapped bead). Another way to get information about the trap force is studying the Brownian movement of a trapped particle as it is explained in section 3. Both the histogram of the Brownian motion or its power spectrum can be used to get the trap parameters.

Single trap calibration has been well studied, but the extension to multiple trap calibration is not immediate in most cases. Multiple trap calibration requires an imaging device and a tracking algorithm to follow the particle path. A recent publication [10] reports multiple trap calibration by potential well reconstruction applying controlled drag forces and using video tracking for measuring the trapped particles position. Another work [11] compares the displacement obtained with a four quadrant detector (commonly used in optical tweezers calibration) with a high-speed camera (2kHz), getting similar performances, and finally power spectrum calibration using a high speed camera has recently been achieved [12]. However video calibration based on Brownian motion analysis with a conventional lab equipment (slow camera) has not been reported yet, to our knowledge Our aim in this work is to use just a CCD camera with moderate capturing frame rates in order to calibrate optical traps by reconstructing the optical potential from the Brownian movement histograms. Once it has been tested with single optical trap calibration, the extension to multiple traps is immediate.

2. Path measurements

In order to calibrate an optical trap by studying the Brownian movement of a trapped particle it is necessary to accurately measure the particle path. This can be done precisely with back focal plane interferometry using a QPD detector, but this method only allows single trap calibration. Video analysis is indispensable in the case of an arbitrary number of traps. In that case, a tracking software is necessary to locate the centre of mass of each particle for each frame, and reconstruct the particle path.

2.1 Position detection by particle tracking

A particle tracking software [13] programmed in LabView with the IMAQ-Vision library has been used to reconstruct the XY-path of the particles from a video recording of its Brownian movement. This program is based on [14] and makes the image processing steps summarized in figure 1. The final result from a sequence of video frames is the XY-path of each particle with sub-pixel resolution.

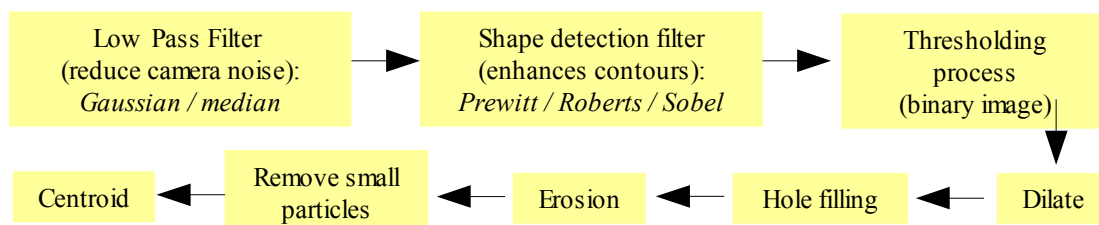


Figure 1. Image processing steps for particle center of mass detection. For each recorded frame, a low pass filter is applied to reduce the camera noise. A shape detection nonlinear filter accentuates the contours of the objects. The obtained image is converted to a binary image using a threshold value (either manually or automatically chosen). The obtained objects are dilated to ensure that all the contours define closed shapes, and finally holes are filled. The last steps consist of erode the objects to compensate the previous dilation, remove small particles (due to dust or noise), and finally, calculate the centroid of each particle.

The original program has been modified in order to track the particles in real time, calculating the centroid of the particle every time a frame is registered by the camera. The tracking successfulness depends strongly on the illumination, particle defocus (because of depth fluctuations) or particle size. That's why the modified version of the tracking software allows real time modification of the image processing parameters in order to optimize the efficiency of the tracking for each given experimental conditions before start taking data.

2.2 Calibration of the CCD camera and quantification of the tracking resolution.

The relation between the distances in the image (measured in pixels) and the real distances at the trapping plane must be known before taking data. It has been calibrated by measuring the position given by the tracking software for some controlled particle positions. A particle stuck at a cover-slip (dry sample) was tracked while the sample was moved in XY by a piezo stage (piezosystem jena xyz-positioner with NV40/3CLE closed loop control). The linear relation between the distance in pixels and the real distance was found to be $0.0462 \pm 0.0001 \mu\text{m}/\text{pixel}$ which fits quite well with the nominal value ($0.0465\mu\text{m}/\text{pixel}$) obtained from the pixel size ($4.65\mu\text{m}$) and the oil immersion objective magnification (100X).

The tracking noise should be previously quantified to ensure that we can actually resolve the thermal agitation in our experimental conditions. Again some still $1\mu\text{m}$ particles (dry sample) were tracked with the LabView program for 2 minutes obtaining a mean standard deviation of 0.15 pixels, which corresponds to a noise around 7 nm in the tracked particle positions. Therefore seems like we have enough resolution to track the Brownian movement in a trap which has a typical range of tenths of nanometers (depending on the trapping power).

2.3 Back Focal Plane Interferometry

This is a commonly used precise method for measuring the particle position [15]. When the laser beam passes through the sample, part of the light is scattered by the particle, and part of the light is not affected. The scattered and non-scattered waves interfere with each other and the resulting interference pattern depends exclusively on the relative position between the particle and the trap center. If we collect the transmitted light with a condenser, at its back focal plane we will have interference rings that will move with the particle (although it is not an image of the particle, but the Fourier Transform). When the particle moves in the XY plane, the scattered wave in the Fourier plane is not modified except for a linear phase, which will make the interference pattern move. The interference pattern is imaged to a QPD detector (Quadrant Photo Diode) which is described in figure 2.

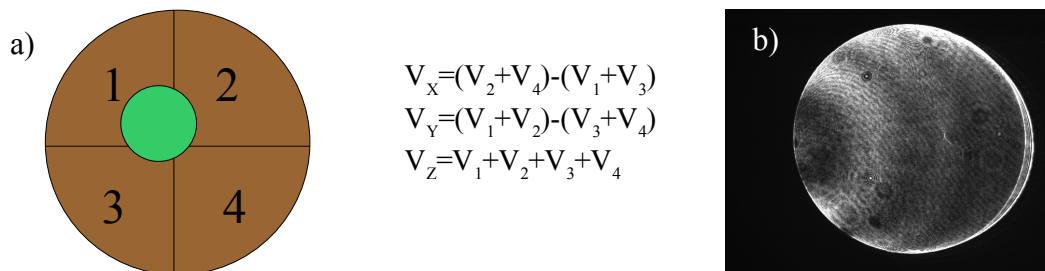


Figure 2. a) QPD diagram, with laser spot. A quadrant photo detector gives V_x , V_y and V_z signals from the differences of light intensity detected in its four quadrants, detecting the movement in the interference pattern. The size of the light spot (which depends on the imaging lens position) affects the sensibility and displacement ranges that can be seen by the detector. b) Interference pattern at the condenser back focal plane. The central spot is located at the left, indicating a particle displacement from the trap center.

This interference pattern is strongly dependent on the relative position of the scattering particle and the rest of the beam, and we can use it to detect the particle position. The QPD is able to detect the intensity variations due to the particle Brownian movement, and give us an electronic

measurement which is proportional to the x and y coordinates of the trapped bead. Data acquisition from the QPD is carried out with a National Instruments acquisition card (NI-DAQ SCB-68), controlled with LabView.

2.4 Time resolution.

QICAM Qimaging camera collects images at a default frame rate of 10 fps with full resolution, although it can work considerably faster if we restrict the detection in a smaller region of interest (ROI), e.g. the size of a single particle. Usually it is better to have high recording rates in order to spend less time for the calibration and be sure that all parameters remain constant. If more speed is needed, pixel binning (2x2, 4x4 or 8x8) can also be activated to reduce the capture time, but then spatial resolution decreases. There is a trade-off between the spatial resolution, which is necessary for having successful tracking, and the time we want to spend in the calibration. It has been observed by measuring a still particle that the tracking noise grows with the binning. Calibration experiments carried out using binning greater than 2x2 give bad results (very noisy trap histograms).

The developed LabView program for real time acquisition, tracking and calibration works at a default rate of 10Hz. When ROI is activated it can work faster than 60Hz, or more than a hundred Hz if we use also 2x2 binning. Even so, for a concrete calibration method explained in section 3.2 (power spectrum analysis), high recording rate is mandatory (typically 20kHz) for being able to retrieve all the necessary spectral information from the collected data. In that case conventional CCD cameras are not useful, only high bandwidth detectors like QPD will work.

3. Force calibration methods

Two calibration methods have been implemented in the lab during the course of this work. Both of them are based in Brownian motion analysis. The first one is the method we want to develop for multiple trap calibration (optical potential reconstruction with video tracking). The second one is the power spectrum analysis which usually gives very good trap stiffness measurements.

3.1 Optical potential reconstruction in Boltzmann statistics

An optically trapped bead in thermal equilibrium moves randomly within the optical trap. The natural Brownian movement is confined in the trap region, near the objective focus. We are going to consider a two-dimensional (x,y) movement which is what we can see observing the sample with a video camera. Thermally driven position fluctuations can give us information on the trapping potential, and we can use them to calibrate the optical trap [16]. In equilibrium we expect the probability density of the particle position to be established by Boltzmann statistics. Then the probability density of finding a molecule or a small particle in a certain position (x,y) position within a potential $U(x,y)$ should be

$$\rho(x, y) = C \exp\left(\frac{-U(x, y)}{k_B T}\right), \quad (1)$$

where k_B is the Boltzmann constant, T is the absolute temperature, and C is a normalization constant. The intuitive explanation of this behaviour is that Brownian particles spend more time in positions where the optical potential energy is lower. If we take an statistically significant number of position measurements and calculate the histogram $h(x,y)$, we expect it to be proportional to the spatial probability density described in (1). The potential experienced by the particle can then be estimated from the histogram: $U(x,y) = -k_B T \ln[h(x,y)] + k_B T \ln C$. Notice that the last term in this equation is just a potential offset which can be neglected. Once we have statistically reconstructed the trap potential we can fit it to a model in order to obtain some characteristic parameters of the trap.

The force field of an optical trap can be assumed to be conservative (force only depends on the relative position of the bead and the laser beam). Trap potential is usually modeled as a harmonic potential because according to several optical trap models the trapping force scales linearly with the bead position near the trap center (spring-like force). In a two-dimensional problem (like our video analysis) the potential model will be:

$$U(x, y) = \frac{1}{2}k_x(x-x_0)^2 + \frac{1}{2}k_y(y-y_0)^2, \quad (2)$$

where k_x and k_y , are the trap stiffness's in the axis directions, and (x_0, y_0) is the equilibrium position. Trap stiffnesses in the two transversal directions are expected not to be exactly the same because of depolarization effects produced by the high numeric aperture of the microscope objective. In order to characterize the trap potential in the harmonic approximation, we need to measure the two transversal stiffness's. By introducing (2) in (1) we obtain the following probability density:

$$\rho(x, y) = C e^{-\frac{k_x}{2k_B T}(x-x_0)^2} e^{-\frac{k_y}{2k_B T}(y-y_0)^2}. \quad (3)$$

The obtained 2D Gaussian function can be separated in two independent dimensions: if we have an (x, y) data array and we calculate the x and y histograms separately, $h_x(x)$ and $h_y(y)$, we should obtain the following relation.

$$h_x(x) \propto \rho_x(x) = \int_{-\infty}^{+\infty} \left(C e^{-\frac{k_x}{2k_B T}(x-x_0)^2} e^{-\frac{k_y}{2k_B T}(y-y_0)^2} \right) dy = C' e^{-\frac{k_x}{2k_B T}(x-x_0)^2}, \quad (4)$$

where C' is the new proportionality constant (notice that the integration of the y-Gaussian in its full domain gives a constant value). According to expression (4) (which can be deduced similarly for $h_y(y)$), the experimental X and Y histograms should have Gaussian shape: $\phi_{\mu, \sigma}(x) = A \exp(-(x-\mu)^2/2\sigma^2)$, where μ is the mean value, σ is the standard deviation, and A is a normalization factor. Identifying terms, we get:

$$k_x = \frac{k_B T}{\sigma_x^2}, \quad k_y = \frac{k_B T}{\sigma_y^2}, \quad x_0 = \mu_x, \quad y_0 = \mu_y, \quad (5)$$

which is an easy way to calculate the trap stiffness's and the central position with just simple statistic calculations. This relations can be very useful to get a fast estimation of the trap parameters in real time. However, the results are not very accurate because the harmonic model (and thus the Gaussian probability distribution) fails for particle positions far from the center. If we take all the data points for making the Gaussian statistics we usually get with (5) softer trap stiffnesses than other methods. For more accurate measurements it is preferable to reconstruct the potential as showed in (2), fitting a parabola just in the central region of the trap potential, where we can actually say that the potential is harmonic, and get the trap parameters.

The outer part of the potential cannot fit the harmonic model because the force loses its linearity with displacement away from the centre [5]. However, this non-harmonic region of the optical potential is also interesting to know information about the force in the outer part of the trap. There the force is not linear with the distance so cannot characterize it with just a stiffness parameter, but we can do from the potential. The optical potential reconstruction using Boltzmann statistics can be used to describe any continuous optical trapping landscape in the region accessible by thermal agitation, and the only necessary parameter is the sample temperature.

3.2 Power spectrum analysis.

The power spectrum analysis of the trapped particle Brownian movement [17] is a precise method for obtaining the trap stiffness from a path measurement. As it is explained in this section, high temporal resolution is needed to have enough information in the Fourier space. Position data can be experimentally obtained by using back focal plane interferometry [15] and a QPD detector. The QPD output signal is not given in nm but in volts, but we will see that it can be self-calibrated fitting the obtained data to a theoretical model if we know the Temperature and the local viscosity. According to Einstein–Ornstein–Uhlenbeck theory of Brownian motion [17], a bead in a harmonic potential within an optical trap can be obtained by solving Langevin equation:

$$m \ddot{x}(t) = -k_{trap}x - \gamma \dot{x}(t) + \sqrt{2k_B T \gamma} \zeta(t) ,$$

where the trap force is modelled as a restoring force (with k_{trap} stiffness) and γ is the Stokes drag constant ($\gamma=3\pi\eta d$, where η is the medium viscosity and d is the particle diameter). The last term of the equation represents the thermal random force which makes the particle oscillate when it is floating within a fluid at temperature T (k_B is the Boltzmann constant). The noise term $\zeta(t)$ is white (temporally uncorrelated) and Gaussian. If we solve this equation [17] by Fourier-transforming it we find that the particle path should have a power spectrum described by a Lorentzian function,

$$P^{exp}(f) = \frac{D^{exp}/(2\pi^2)}{f_c^2 + f^2} \quad f_c = \frac{k_{trap}}{2\pi\gamma} ,$$

whose shape is related with the system parameters. This function is almost constant for low frequencies (plateau) but starts decreasing (like f^{-2}) from the corner frequency (f_c). If we fit it to the experimental power spectrum we obtain f_c which is related with the trap stiffness, and D^{exp} (in QPD units: V^2/s) which can be used to retrieve the QPD calibration constant (m/volts) comparing it with the nominal diffusion coefficient $D=k_B T/\gamma$ (m^2/s).

The main limitation of this method is that needs high temporal resolution data to have enough spectral information. Therefore it cannot be carried out with conventional CCD cameras, but high bandwidth detectors are necessary (QPD, PSD, ultrafast cameras), and most of them (except for the ultrafast cameras) cannot measure more than one trap. A possible error source of this method are the local parameters like medium viscosity, particle diameter and temperature that must be known for the system parameters calculations. A MATLAB program [18] has been used to calibrate the trap constant by power spectrum analysis directly from QPD measurements.

4. Setup

An holographic optical tweezer has been built. The optical system is showed in figure 3. Holography is necessary to have the control of multiple traps. The setup includes a commercial inverted microscope (Nikon TE2000-E) with an oil immersion objective (Nikon 100X, 1.30NA, 0.2mm working distance) which is used for both focusing the trapping light on the sample and looking at it. The beam should be adequately resized, collimated and codified before entering the microscope objective, with a fine alignment of the optical elements.

4.1 Beam conditioning

The trapping beam is generated with a Nd:YVO₄ IR laser (Viasho, 500mW, 1064nm). The laser light is expanded with a microscope objective ($f=7.5mm$) and the speckle is filtered with a

pinhole. The expanding filtered beam is then collimated with a lens and sent to a spatial light modulator (Hammamatsu LCOS-SLM X10468, only-phase modulation) which will imprint the desired phase pattern on the reflected light beam. The holograms are calculated and sent to the SLM by the HoloTrap software [8], which also corrects the aberrations due to SLM lack of flatness adding an additional phase map to the desired holograms. A half-wavelength plate was introduced at the output of the laser to rotate the polarization direction until the optimum modulation efficiency in the SLM was achieved. The codified beam (16x12mm) is then resized with a 1/3 magnification telescope to fit the microscope entrance pupil (4.9mm). A trade off between slightly overfill the entrance pupil [19] without losing too much light was taken into account.

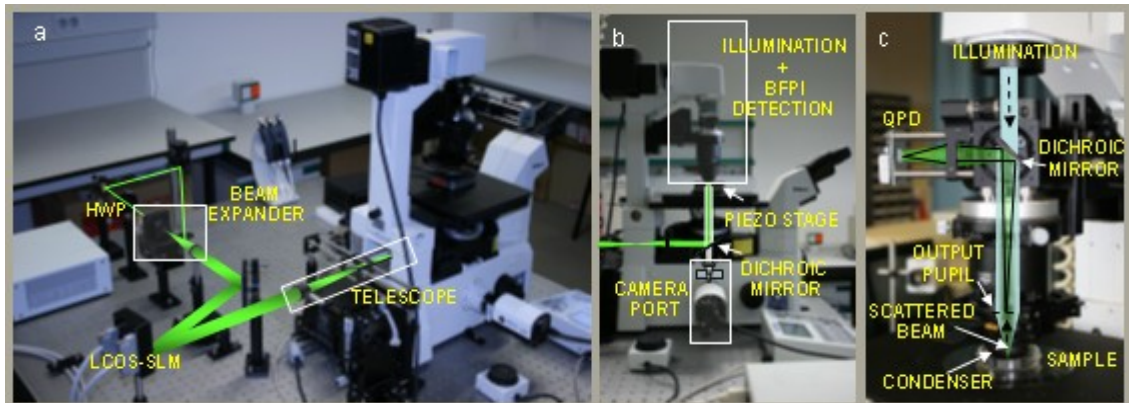


Figure 3. Optical setup. In a) beam conditioning (polarizing rotation, expansion, codifying and resizing) is showed. In b) the trapping beam path and the imaging path inside the microscope are appreciated. In c) illumination through the condenser and Back Focal Plane Interferometry setup are shown. An oil immersion condenser in contact with the sample (covered with a cover-slip) collects the laser light (both the light scattered by the particle and the non scattered light). An interference pattern is generated at the condenser back focal plane, and this pattern is imaged to the QPD surface with a lens. A dichroic mirror enables the back focal plane interferometry measurement while the microscope illumination path remains operative.

4.2 Inside the microscope: trapping, imaging, illumination and back -focal-plane detection

The microscope configuration makes possible both the sample observation through the camera port (using the microscope illumination, which can be bright field or phase contrast) and particle trapping by introducing a laser beam through the fluorescence port. Inside the microscope, the incoming laser is reflected by a dichroic mirror and redirected to the objective where it is focused in the sample plane. Under the dichroic mirror a CCD camera (Qimaging QICAM 12-bit Mono Fast 1394) records the image of the trapping plane. The system is aligned for making the trapping plane and the observation plane coincide.

The last part of the setup is the one that makes possible the back-focal-plane displacement detection. As it can be seen in figure 3c it consists of an oil immersion condenser (1.4 NA) that collects the scattered light (the same condenser used for the sample illumination), a dichroic mirror (which lets the microscope illumination pass through but reflects the laser light), and a quadrant photo diode (QPD) which is able to measure the trapped bead position with high spatial and temporal resolution. The QPD is placed at a conjugate plane of the condenser output pupil (figure 3c). The size of the laser spot on the QPD can be adjusted by moving the imaging lens until we get the desired response.

4.3 The sample

Polystyrene spheric particles have been used to calibrate the force applied by the optical trap. To calibrate the trap force it is necessary to measure the particle position while it thermally

oscillates. Experiments have been done with $1\mu\text{m}$ diameter spheres. Particles were suspended in sodium dodecyl sulfat (SDS) solution of 0.35g/L . According to [20] for that SDS concentration (0.0012M) the viscosity of the medium will be around 1.01 times the water viscosity ($10^{-3}\text{Pa}\cdot\text{s}$), that is $1.01\text{mPa}\cdot\text{s}$. The sample was placed in a cover-slip on the microscope objective with immersion oil between the glass and the objective.

5. Results and discussion

Once we have measured the particle 2D-movement within the trap (with both QPD and video tracking), we are ready to calibrate the optical trap obtaining its transversal stiffness.

5.1 Calibration from histograms

X and Y position histograms have been measured both with a QPD (back-focal-plane interferometry) and a CCD camera (video tracking) in order to compare their performance in the same experimental conditions: $1\mu\text{m}$ bead trapped at $4\mu\text{m}$ height from the cover-slip with 4mW laser power at the sample. The QPD results describe almost an ideal Gaussian, thanks to the huge amount of data ($2\cdot 10^6$ points) that can be collected in only 10 seconds. The video capture and tracking is much slower (10^4 points for an almost 3 minutes long measurement). To compensate the lower number of data points the experiment has been repeated several times in the same experimental conditions and the results have been averaged. The resulting histograms are plotted in figure 4.

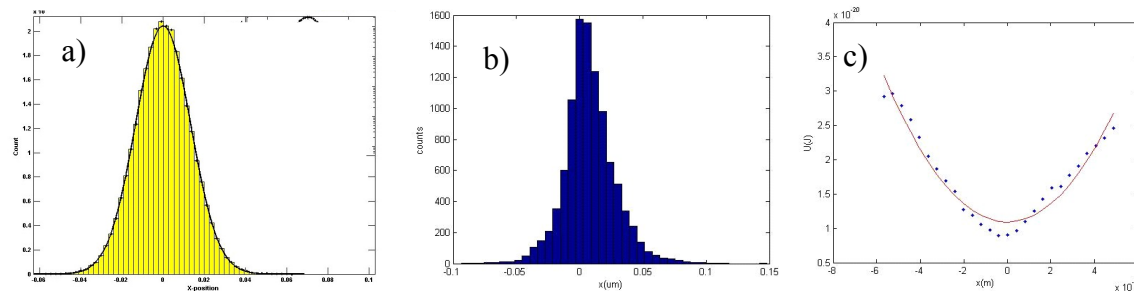


Figure 4. a) x-histogram of a QPD-obtained path b) x-histogram of a video-tracked path. c) Optical potential reconstruction based on data in b.

From QPD-obtained histograms, the calculated x and y trap stiffnesses are $7.8\text{pN}/\mu\text{m}$ and $11.2\text{pN}/\mu\text{m}$. From video tracking we obtained first a fast real time estimation of the trap stiffness from the standard deviation of positions ($\sigma_x=53\text{nm}$ and $\sigma_y=57\text{nm}$, which somehow reflect the size of the trap). Then the trap potential (figure 4c) was reconstructed from the histogram by taking into account only the central part of the trap (1σ) which is the harmonic region.

5.2 Calibration from power spectrum

For the same experimental conditions, the data obtained with the QPD has been used to measure more precisely the trap parameters by power spectrum analysis. In the taken spectra there is a systematic presence of noise peaks (probably due to electronic noise, the SLM refresh rate, laser pulsation, etc.). Those peaks are clearly out of the expected Lorentzian behaviour and they can be filtered (or at least attenuated) using a median filter. The obtained X-spectrum and the corresponding Lorentzian fit are shown in figure 5. The fitted Lorentzians had a corner frequency of 218Hz and 227Hz respectively for X and Y movements. The trap parameters for each method are summarized in table 1.

We observe that the trap stiffness's obtained from harmonic fitting of k using the video tracking data differ 6% and 9% respect to the k_x and k_y values obtained from QPD histograms. The tracking results are better when points from the non-harmonic region are eliminated. Probably this difference is introduced by the significant difference in the number of data points of each measurement. A observable difference also reported in [16] is that trap calibration based on histogram analysis always tend to give weaker trap stiffness's than power spectrum analysis (which seems to be the most reliable method). In power spectrum measurements external noise is clearly distinguishable (low frequency noise if the optical table is not inflated, electronic peaks at discrete frequencies, or high frequency noise), and we can filter them keeping the Lorentzian shape. But in the case of histogram measurements the experimental noise just makes the Gaussian wider, and it's difficult to quantify and separate the noise from the real data. This method is probably more sensible to external noise than other ones.

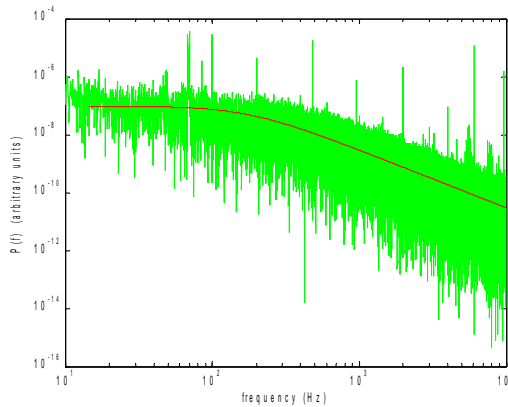


Figure 5. Rough x-power spectrum and fitted Lorentzian function

Table 1. Summary of trap parameters measured with different methods in x and y directions

Direction	Video tracking		QPD	
	Fast k estimation (from σ)	k from harmonic potential (1σ near the trap center)	k from histogram (Gaussian fit)	k from Power Spectrum (Lorentzian fit)
X	7.5 ± 0.3 pN/ μm	8.3 ± 0.5 pN/ μm	7.8 pN/ μm	12.9 pN/ μm
Y	8.5 ± 0.8 pN/ μm	10.2 ± 0.5 pN/ μm	11.2 pN/ μm	13.4 pN/ μm

6. Conclusions

A video force calibration method has been developed and implemented in a holographic optical tweezers setup. A LabView program has been developed for real-time calibrate single or multiple optical traps using a particle tracking algorithm. The proposed method gives trap stiffnesses similar to those obtained with QPD histogram measurements, but lower than those obtained from power spectrum analysis. Video tracking is slower and less precise than QPD, but it could be an easy way to estimate optical trap stiffnesses in multiple trap experiments. A difference with other methods is that the optical potential reconstruction based on histogram is also applicable in non harmonic optical potentials, because we can measure actually any kind of optical landscape accessible by thermal agitation. Another advantage is that the only experimental parameter that must be known is temperature, there is no need to know other sample parameters like medium viscosity, distance to the cover-slip, or particle size because one is directly measuring the thermal agitation of the trapped bead.

To make this method competitive as a force calibration technique it will be necessary to improve the particle tracking resolution, adjusting better the experimental illumination levels but also the threshold values, and choosing carefully the applied image processing filters. A

way to quantify the noise of each measurement should be taken into account, for example observing the statistical deviations of the histogram from an ideal Gaussian shape, trying to overcome the experimental histogram widening. Real time multiple trap calibration would be then as simple as executing the software connected to the microscope camera, multiple trap experiments could be carried out with simultaneous force measurements in each trap. An interesting further improvement of this method is the measure of the z coordinate of the particles by quantifying the defocus of each particle with image processing. That will enable z force calibration, and thus three-dimensional force measurements.

Acknowledgements

I thank, Prof. Artur Carnicer for his help and encouragement throughout the course of this work, I thank Mireia Rosado for providing the tracking algorithm and I also thank the rest of people from Grup de Recerca en Optica Física for their valuable help and comments.

References

- [1] Lang M J and Block S M 2003 Resource letter: LBOT-1: laser-based optical tweezers. *Am. J. Phys.* **71**(3), 201–215
- [2] Ashkin A 1970 Acceleration and trapping of particles by radiation pressure *Phys Rev Lett* **24**, 156-159
- [3] Ashkin A, Dziedzic J M, Bjorkholm J E and Chu S 1986 Observation of a single-beam gradient force optical trap for dielectric particles *Opt. Lett.* **11**, 288-290
- [4] Ashkin A 1992 Forces of a single-beam gradient laser trap on a dielectric sphere in the ray optics regime *Biophysical Journal* **61**, 569-582
- [5] Harada Y and Asakura T 1996 Radiation forces on a dielectric sphere in the Rayleigh scattering regime *Opt. Commun.* **124**, 529-541
- [6] Gouesbet G, Maheu B and Gréhan G 1988 Light scattering from a sphere arbitrarily located in a Gaussian beam, using a Bromwich formulation *J. Opt. Soc. Am. A.* **5**, No. 9, 1427-1443 (1988).
- [7] Curtis J E, Koss B A and Grier D G 2002 Dynamic holographic optical tweezers *Opt. Commun.* **207**, 169-175
- [8] Pleguezuelos E, Carnicer A, Andilla J, Martín-Badosa E and Montes-Usategui M 2007 HoloTrap: Interactive hologram design for multiple dynamic optical trapping *Comp. Phys. Commun.* **176** (11-12), 701-709 (2007)
- [9] Neuman K C and Block S M 2004 Optical trapping *Rev. Sci. Instr.* **75**, 2787-2809
- [10] Belloni F, Monneret S, Monduc F and Scordia M 2008 Multiple holographic optical tweezers parallel calibration with optical potential well characterization *Opt. Exp.* **16**, 9011-9020
- [11] Keen S, Leach J, Gibson G and Padgett M J 2007 Comparison of a high-speed camera and quadrant detector for measuring displacements in optical tweezers *J. Opt. A: Pure Appl. Opt.* **9**, S264-S266
- [12] Otto O, Gutsche C, Kremer F and Keyser U F 2008 Optical tweezers with 2.5 kHz bandwidth video detection for single-colloid electrophoresis *Rev. Sci. Instr.* **79** 023710.
- [13] Rosado M 2008 Tracking of multiple samples by video techniques. *GROF-UB Internal Report*.
- [14] The particle tracking resource page (august 2008) <http://faculty.washington.edu/gmilne/tracker.htm>
- [15] Gittes F and Schmidt C F 1998 Interference model for back-focal-plane displacement detection in optical tweezers *Opt. Lett.* **23**, 7-9
- [16] Florint E L, Pralle A, Stelzer E H K and Hörber J K H 1997 Photonic force microscope calibration by thermal noise analysis *Appl. Phys. A* **66**, S75-S78
- [17] Berg-Sorensen K and Flyvbjerg H 2004 Power spectrum analysis for optical tweezers *Rev. Sci. Instr.* **75**, 594-612
- [18] Hansen P M, Tolić-Norrelykke I M, Flyvbjerg H, Berg-Sorensen K 2006 Tweezercalib 2.0: faster version of MatLab package for precise calibration of optical tweezers *Comp. Phys. Commun.* **174** (6), 518-520
- [19] Martín-Badosa E, Montes-Usategui M, Carnicer A, Andilla J, Pleguezuelos E and Juvells I 2007 Design strategies for optimizing holographic optical tweezers set-ups *J. Opt. A: Pure Appl. Opt.* **9**, S267–S277
- [20] Akbas H, Sidim T, Iscan M 2003 Effect of polyoxyethylene chain length and electrolyte on the viscosity of mixed micelles *Turk J. Chem.* **27**, 357-363